

# PHOTOPRODUCTION OF $\pi^0$ MESONS FROM NEUTRONS AROUND THE $N(1518)$ RESONANCE\*

By

Yoshio YOSHIMURA\*\*

Department of Physics, Faculty of Science, Kyoto University, Kyoto  
(Received May 7, 1969)

## ABSTRACT

The experiment on the photoproduction of  $\pi^0$  mesons from neutrons was carried out, by using a liquid deuterium target, at the pion angle of  $90^\circ$  in the center of mass system and in the energy region around the  $N(1518)$  resonance. The reaction  $\gamma+n\rightarrow\pi^0+n$  was identified by detecting the neutron and two  $\gamma$  rays decaying from the  $\pi^0$  meson, with a scintillation counter and a pair of lead glass Čerenkov counters, respectively. The result seems to be consistent with the previous results<sup>1)</sup> that the isovector part is dominant in the  $D_{13}$ -amplitude of the  $\pi$  meson photoproduction on the free nucleon around the  $N(1518)$  resonance, from the measurement of the reaction  $\gamma+d\rightarrow\pi^0+d$ .

## § 1. Introduction

Many theoretical and experimental studies on the pion photoproduction from protons,  $\gamma+p\rightarrow\pi^0+p$  and  $\gamma+p\rightarrow\pi^++n$ , have been performed, because the studies of the reaction provide the valuable informations about the pion-nucleon interaction. Also the information on the electromagnetic interaction of the incoming photon with the nucleon can be obtained by the studies on the pion photoproduction.

In the pion photoproduction from nucleons, the electromagnetic interaction can be expressed with a sum of the isoscalar and isovector interactions, since the final  $\pi N$  system can have either  $I=\frac{1}{2}$  or  $\frac{3}{2}$  state. Using Watson's isospin formalism,<sup>2)</sup> the transition amplitudes of the pion photoproduction can be written as follows:

$$T(\gamma+p\rightarrow\pi^++n)=\sqrt{\frac{1}{3}}\left\{2V_3+\sqrt{\frac{1}{2}}(2S_1+2V_1)\right\}, \quad (1-1)$$

$$T(\gamma+p\rightarrow\pi^0+p)=\sqrt{\frac{1}{3}}\left\{2V_3-\frac{1}{2}(2S_1+V_1)\right\}, \quad (1-2)$$

$$T(\gamma+n\rightarrow\pi^-+p)=\sqrt{\frac{1}{3}}\left\{2V_3-\sqrt{\frac{1}{2}}(2S_1-V_1)\right\}, \quad (1-3)$$

$$T(\gamma+n\rightarrow\pi^0+n)=\sqrt{\frac{1}{3}}\left\{2V_3+\frac{1}{2}(2S_1-V_1)\right\}, \quad (1-4)$$

where  $S_1$  is an isoscalar part of the transition amplitude and  $V_1$  and  $V_3$  are the isovector parts of the transition amplitude, defining by

\* This experimental results were briefly reported as a short note in Journal of Physical Society of Japan.<sup>3)</sup>

\*\* Now at Institute for Nuclear Study, University of Tokyo, Tokyo, Japan.

$$\begin{aligned}
S_1 &= \left\langle I = \frac{1}{2}, I_3 = \pm \frac{1}{2} \left| \mathbf{S} \right| I = \frac{1}{2}, I_3 = \pm \frac{1}{2} \right\rangle, \\
\pm \frac{1}{2} V_1 &= \left\langle \frac{1}{2}, \pm \frac{1}{2} \left| \mathbf{V} \right| \frac{1}{2}, \pm \frac{1}{2} \right\rangle, \\
\sqrt{2} V_3 &= \left\langle \frac{3}{2}, \pm \frac{1}{2} \left| \mathbf{V} \right| \frac{1}{2}, \pm \frac{1}{2} \right\rangle.
\end{aligned}$$

Generally, three amplitudes,  $S_1$ ,  $V_1$ , and  $V_3$ , are functions of ordinary spins and momenta, besides being dependent on the explicit form of the interaction. Similarly, the transition amplitude of the reaction  $\gamma + d \rightarrow \pi^0 + d$  can be written, excluding the deuteron form factor, as follows:

$$T(\gamma + d \rightarrow \pi^0 + d) \propto \sqrt{\frac{1}{3}} \{4V_3 - V_1\}. \quad (1-5)$$

In order to estimate five real parameters, conveniently chosen as the three amplitudes,  $|S_1|^2$ ,  $|V_1|^2$  and  $|V_3|^2$ , and two relative phase angles,  $(\arg V_3 - \arg V_1)$  and  $(\arg V_1 - \arg S_1)$ , five  $\pi$  photoproduction amplitudes of the process (1-1) to (1-5) have to be measured.

Taking account of the  $N(1518)$  resonance for the intermediate state of the process  $\gamma + N \rightarrow N^* \rightarrow \pi + N$ , the isoscalar part  $S_1$  and the isovector part  $V_1$  can contribute to the process. In order to evaluate  $V_1$  and  $S_1$ , three processes, (1-5), (1-1) or (1-2) and (1-3) or (1-4), must be measured.

Previously we have reported<sup>1)</sup> the experimental results of the differential cross section for the reaction  $\gamma + d \rightarrow \pi^0 + d$  at the pion angle of  $50^\circ \sim 60^\circ$  in the center of mass system and in the photon energy range from 500 MeV to 820 MeV. The aim of the experiment was to measure the isotopic vector part of the  $\pi^0$  photoproduction amplitude around the  $N(1518)$  resonance. The results are consistent with the conclusion that the isotopic vector part is dominant in the  $D_{13}$ -wave amplitude of the  $\pi^0$  photoproduction from free nucleons.

A few differential cross sections for the reaction  $\gamma + n \rightarrow \pi^0 + n$  have been measured; G. Cocconi and A. Silverman<sup>2)</sup> measured the ratio of the  $\pi^0$  photoproduction cross sections from deuterium to these from hydrogen at the pion angle of  $90^\circ$  in lab. system around the photon energy of 300 MeV by detecting only one of decay  $\gamma$ -rays from the  $\pi^0$  meson. C. R. Clinesmith et al.<sup>3)</sup> measured also the same ratio at the pion angle from  $0^\circ$  to  $90^\circ$  in the center of mass system and at photon energies of 1150 MeV and 1350 MeV by detecting two  $\gamma$ -rays. They reduced the neutron cross sections from this ratio and the hydrogen cross section.

The present paper reports the experimental result<sup>4)</sup> of the  $\pi^0$  meson photoproduction from neutrons at the pion angle of  $90^\circ$  in the photon-neutron center of mass system around the  $N(1518)$  resonance. The measurement has been carried out by detecting two  $\gamma$  rays decaying from the  $\pi^0$  meson and the recoil neutron, using a liquid deuterium target.

## § 2. Experimental Method

### a. Beam and Target

The general layout of this experiment is shown in Fig. 1. The experiment was carried out with the bremsstrahlung beam from the electron synchrotron of Institute for Nuclear Study, University of Tokyo. The bremsstrahlung beam was produced in a platinum radiator of  $50 \mu$  in thickness which was bombarded with the circulating

electron beam of 950 MeV. The beam was collimated by a 300 mm- thick lead collimator with a hole of 5 mm in diameter. The beam profile was 26 mm in diameter at the position of the target and 30 mm in diameter at a quantameter. The charged particles in the bremsstrahlung beam were swept away by a sweeping magnet behind the collimeter. The beam intensity was measured with the Wilson type quantameter. The fluctuation of the maximum energy of the bremsstrahlung beam was within 25 MeV.

The target container was made of 0.075 mm-thick Mylar. Its shape was cylindrical; 97 mm in length along the beam axis and 50 mm in diameter. The target container was filled with liquid deuterium or liquid hydrogen.

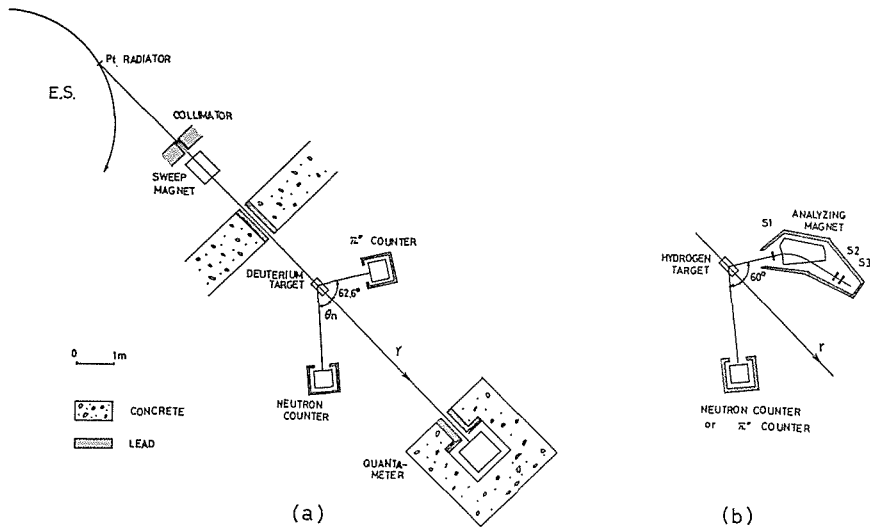


Fig. 1. Experimental layout. (a) The layout for the reaction  $\gamma + n \rightarrow \pi^0 + n$  is shown. (b) The  $\pi^0$  counter or the neutron counter were set for their calibration run.

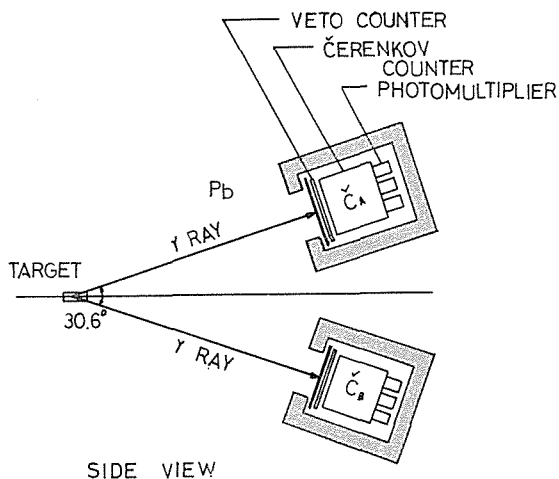


Fig. 2.  $\pi^0$  counter. The opening angle of the Čerenkov counters was set at  $30.6^\circ$  to obtain the maximum detecting efficiency for  $\pi^0$  mesons of 507 MeV/c.

### b. $\pi^0$ Counter

The  $\pi^0$  counter used in this experiment has already been reported<sup>6)</sup>. As is shown in Fig. 2, the  $\pi^0$  counter consisted of a pair of Čerenkov counters of the total absorption type. Their opening angle was set at  $30.6^\circ$  to obtain the maximum detecting efficiency for  $\pi^0$  mesons of 507 MeV/c. In order to reject low energy  $\gamma$  rays and charged particles, a lead sheet of 2 mm and a veto counter made of plastic scintillator of 5 mm in thickness were placed in front of each Čerenkov counter. The lead sheet converts 250 MeV  $\gamma$  rays into charged particles with the probability of 21.2%.

The Čerenkov counters were made of SF-2 lead glass<sup>7)</sup> which has the reflective index of 1.6477, the density of 3.84 g/cm<sup>3</sup> and a radiation length of 10.9 g/cm<sup>2</sup>. The shape was a cube of 250 mm. The lead glass was viewed by nine photomultipliers (RCA 6655A) from one side. After nine output pulses were adjusted to give the same pulse heights, they were added together. The pulse height linearities, the energy resolutions and the detecting efficiencies of the Čerenkov counters were measured in the energy region from 100 MeV to 700 MeV by using the electron beam of the momentum spread of about 2%. The results are shown in Fig. 3.

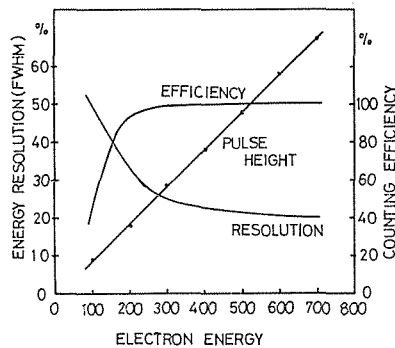


Fig. 3. Pulse height linearity, energy resolution and detecting efficiency counter of the Čerenkov

The detecting efficiency of the  $\pi^0$  counter was obtained by measuring  $\pi^0$  mesons produced from the reaction  $\gamma + p \rightarrow \pi^0 + p$ . The experimental layout is shown in Fig. 1(b). In order to determine the momentum and intensity of  $\pi^0$  mesons, the recoil proton was detected by the combination of the momentum analyzing magnet and the time of flight method. S1 counter extended the angle from  $58.0^\circ$  to  $62.0^\circ$  in the Lab. system. The flight time between the counter S1 and S2 was measured by using the time to pulse height converter. The momentum spread of the analyzing magnet was 6.73%. The electronic system is shown in Fig. 4(a). As is shown in the Table 1, the measured detecting efficiencies agree well with the values which are calculated geometrically with the assumption that the detecting efficiencies of the Čerenkov counters are 100% for  $\gamma$  rays.

### c. Neutron Counter

The construction of the neutron counter is shown in Fig. 5. In order to reject low energy  $\gamma$  rays and charged particles, a lead sheet of 3 mm in thickness and a veto counter made of a plastic scintillator of 10 mm in thickness were placed in

Table 1. Detecting efficiency of  $\pi^0$  counter.

energy of $\pi^0$ (MeV)	measured value (%)	calculated value (%)
$510 \pm 60$	$1.06 \pm 0.19$	1.12
$605 \pm 65$	$0.89 \pm 0.30$	0.91

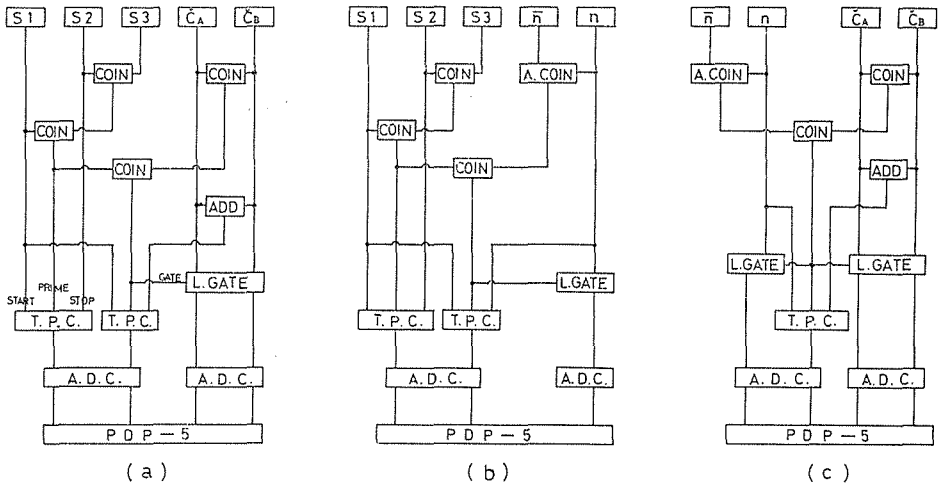


Fig. 4. Electronic systems used for this experiments. (a), (b) and (c) are the electronic systems for the  $\pi^0$  counter calibration run, the neutron counter calibration run and the measurement of the reaction  $\gamma + n \rightarrow \pi^0 + n$  run, respectively. The abbreviations are as follows:

- L. Gate : The linear gate
- T.P.C. : The time to pulse height converter
- A.D.C. : The analog to digital converter
- PDP-5 : The data prosesser

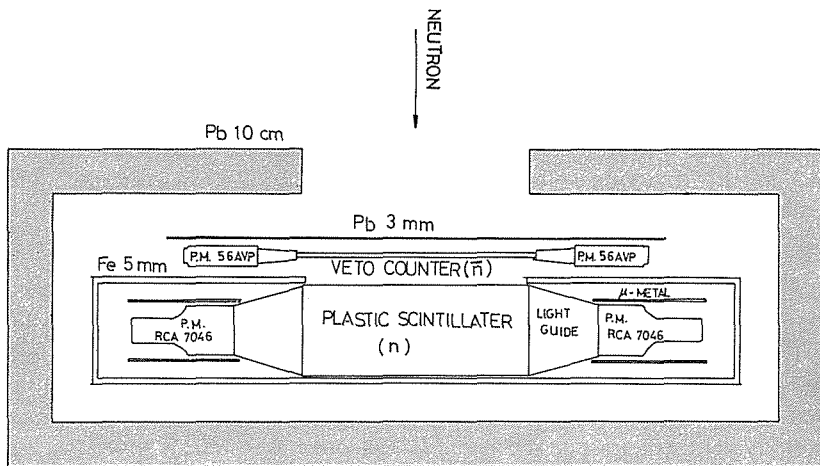


Fig. 5. Construction of the neutron counter.

front of the neutron counter. The neutron counter was made of a plastic scintillator<sup>9)</sup> of 20 cm × 50 cm × 20 cm (width × height × thickness). The plastic scintillator was viewed by two RCA 7046 photomultipliers through the Lucite light guides. The dependence of the pulse height on the positions in the plastic scintillator was measured by moving a light pulser or the electron beam. The maximum fluctuation of the pulse height was found to be about 2%.

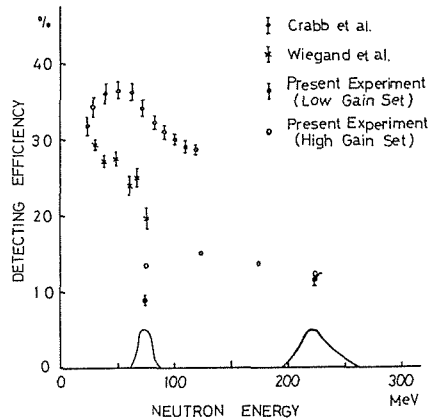


Fig. 6. Detecting efficiency of the neutron counter. The neutron counter of Crabb et al.<sup>9)</sup> was 28.6 cm in thickness. The bias level was set at 6 MeV of the protons. The counter of Wiegand et al.<sup>9)</sup> was 15 cm in thickness. The bias level was set at 4 MeV. Our counter was 20 cm in thickness. The bias level was set at 45 MeV for the low gain set. Two solid curves show the energy spread of the neutron used for the calibration run at 75 MeV and 225 MeV, respectively.

The detecting efficiency of the neutron counter was measured by using the neutrons produced from the reaction  $\gamma + p \rightarrow \pi^+ + n$ . In order to determine the energies and the intensity of neutrons, the  $\pi^+$  mesons were detected with the same apparatus used in the  $\pi^0$  counter calibration run. The electronic system used in this run is shown in Fig. 4(b). The detecting efficiencies of the neutron counter were measured for two sets of the counter gain. The detecting efficiencies for the high gain and low gain sets together with other results<sup>9)</sup> are shown in Fig. 6 and Table 2. It is seen that the detecting efficiencies of our counter are fairly lower than others', because the bias was set at higher level and corresponded to 45 MeV of protons for the low gain set. At the neutron energy of 225 MeV the detecting efficiency for the high gain set is nearly equal to that for the low gain set. The pulse height distribution obtained with the low gain set is shown in Fig. 7.

#### d. Reaction $\gamma + d \rightarrow \pi^0 + n + (p)^*$

The differential cross section of the reaction  $\gamma + n \rightarrow \pi^0 + n$  was measured with the  $\pi^0$  counter and the neutron counter by using the deuterium target, as is shown in Fig. 1. In order to reduce the background of the low energy neutron produced from the photodisintegration of the deuteron, the low gain set of the neutron counter was used during this run. The intensity of the  $\gamma$  ray beam was kept less than about  $5 \times 10^8$  equivalent quanta per second. The electronic system is shown in Fig. 4(c).

\* (N) denotes the spectator nucleon, hereafter.

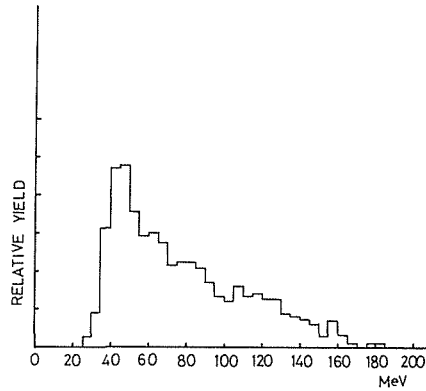


Fig. 7. Pulse height distribution of the neutron counter for 225 MeV neutron. The energy scale of the abscissa corresponds to the energy of proton.

Table 2. Detecting efficiency of the neutron counter.  
(low gain set)

energy of neutron (MeV)	efficiency (%)
$75 \pm 8$	$9.1 \pm 0.6$
$225 \pm 18$	$11.5 \pm 0.6$

For each event, the pulse heights of the neutron counter and both the Čerenkov counters and the flight time of the neutron were measured in coincidence and recorded with a PDP-5 data processor. The flight time of the neutron was measured by detecting the time difference between the pulses from the Čerenkov counters and the pulse from the neutron counter. As is shown in Fig. 1, the  $\pi^0$  counter was set at  $62.6^\circ$  in the Lab. system. The neutron counter was set at  $\theta_n = 34.8^\circ, 38.0^\circ, 41.2^\circ$  and  $47.6^\circ$  in the Lab. system. The setting of  $\theta_n = 41.2^\circ$  corresponds to  $\theta_{\pi}^{\text{CM}} = 90^\circ$  and  $k' = 750$  MeV where  $\theta_{\pi}^{\text{CM}}$  denotes the angle of the produced  $\pi^0$  meson in the center of mass system.  $k'$  denotes the energy of the incident  $\gamma$  ray in the system in which the target neutron is at rest.

### § 3. Data Reduction

#### a. Cross Section Formulas

Since the deuterium was used as the target of the reaction  $\gamma + n \rightarrow \pi^0 + n$ , the derivation of the cross section from the yield is rather complicated. The solid angle in the center of mass system can not be evaluated by the usual means because of the internal motion of the neutron in the deuteron. In the present paper the cross section was calculated by using the Monte Carlo method. It was assumed that each target neutron has the momentum distributions expected from the Hulthén wave function<sup>10)</sup> and that a  $\gamma$  ray interacts with only one nucleon, leaving the other as it is (spectator model). The calculations were performed by a computer HITAC 5020. The procedure of the calculation is as follows:

The number of the detected events per unit equivalent quanta caused by the  $\gamma$  rays with the energy between  $k$  and  $k + \Delta k$  and the neutrons with the initial momentum between  $\mathbf{P}$  and  $\mathbf{P} + \Delta \mathbf{P}$  is given by

$$Y(k, \mathbf{P}) \Delta \mathbf{P} \Delta k = \frac{d\sigma}{d\Omega^{\text{CM}}} \cdot \Delta \Omega^{\text{CM}}(\mathbf{q}) \cdot N_r(k) \Delta k \cdot N_t(\mathbf{P}) \Delta \mathbf{P} \cdot \eta_N \cdot \eta_{\pi^0}(\mathbf{q}), \quad (3.1)$$

where

- $\frac{d\sigma}{d\Omega^{\text{CM}}}$  : The differential cross section in the center of mass system.  
 $\Delta \Omega^{\text{CM}}(\mathbf{q})$  : The solid angle in the center of mass system which is calculated by taking account of the internal motion of the target neutron.  
 $N_r(k) \Delta k$  : The number of the  $\gamma$  rays with the energy between  $k$  and  $k + \Delta k$  per unit equivalent quanta.  
 $N_t(\mathbf{P}) \Delta \mathbf{P}$  : The number of the target neutron with the momentum between  $\mathbf{P}$  and  $\mathbf{P} + \Delta \mathbf{P}$  per  $\text{cm}^2$ .  
 $\eta_N$  : The detecting efficiency of the neutron counter  
 $\eta_{\pi^0}(\mathbf{q})$  : The detecting efficiency of the  $\pi^0$  counter.  
 $k$  : The energy of the incident  $\gamma$  rays in the Lab. system  
 $\mathbf{P}$  : The initial momentum of the target neutron in the Lab. system.  
 $\mathbf{q}$  : The momentum of the produced  $\pi^0$  meson in the Lab. system.

$\Delta \Omega^{\text{CM}}(\mathbf{q})$  and  $\eta_{\pi^0}(\mathbf{q})$  depend on  $k$  and  $\mathbf{P}$  through  $\mathbf{q}$ . The number of events per unit equivalent quanta is obtained by integrating  $Y(k, \mathbf{P})$  as follows :

$$\begin{aligned}
 Y &= \int_{k=0}^{k_{\text{max}}} \int_{\mathbf{P}} Y(k, \mathbf{P}) d\mathbf{P} dk, \\
 &= \int_{k=0}^{k_{\text{max}}} \int_{\mathbf{P}} \frac{d\sigma}{d\Omega^{\text{CM}}} \cdot \Delta \Omega^{\text{CM}}(\mathbf{q}) \cdot \eta_N \cdot \eta_{\pi^0}(\mathbf{q}) \cdot N_t(\mathbf{P}) d\mathbf{P} \cdot N_r(k) dk, \\
 &= \frac{d\bar{\sigma}}{d\Omega^{\text{CM}}} \eta_N \cdot \int_{k=0}^{k_{\text{max}}} \int_{\mathbf{P}} \Delta \Omega^{\text{CM}}(\mathbf{q}) \cdot \eta_{\pi^0}(\mathbf{q}) \cdot N_t(\mathbf{P}) d\mathbf{P} \cdot N_r(k) dk, \\
 &= \frac{d\bar{\sigma}}{d\Omega^{\text{CM}}} \eta_N \cdot R(k, \mathbf{P}), \quad (3.2)
 \end{aligned}$$

where

$$R(k, \mathbf{P}) = \int_{k=0}^{k_{\text{max}}} \int_{\mathbf{P}} \Delta \Omega^{\text{CM}}(\mathbf{q}) \cdot \eta_{\pi^0}(\mathbf{q}) \cdot N_t(\mathbf{P}) d\mathbf{P} \cdot N_r(k) dk, \quad (3.3)$$

$d\bar{\sigma}/d\Omega^{\text{CM}}$  is the average of the differential cross section with the energy region determined by the experimental arrangement.  $R$  was calculated by the Monte Carlo method which will be described as follows:

(a) The reactions due to the  $\gamma$  rays of less than 500 MeV were not detected kinematically with our experimental arrangement. In order to take account of the bremsstrahlung spectrum the energy region between 500 MeV and 950 MeV ( $=k_{\text{max}}$ ) was divided into 40 parts in which the equal number of the  $\gamma$  rays were contained. Accordingly,  $R$  can be expressed as follows:

$$\begin{aligned}
 R(k, \mathbf{P}) &= \sum_{i=1}^{40} \int_{\mathbf{P}} \Delta \Omega^{\text{CM}}(\mathbf{q}) \cdot \eta_{\pi^0}(\mathbf{q}) \cdot N_t(\mathbf{P}) d\mathbf{P} \cdot N_r(k_i) \Delta k_i, \\
 &= n_r \sum_{i=1}^{40} R_i, \quad (3.4)
 \end{aligned}$$

where

$$\begin{aligned}
 n_r &= N_r(k_i) \Delta k_i, \\
 R_i &= \int_{\mathbf{P}} \Delta \Omega^{\text{CM}}(\mathbf{q}) \cdot \eta_{\pi^0}(\mathbf{q}) \cdot N_t(\mathbf{P}) d\mathbf{P}. \quad (3.5)
 \end{aligned}$$



$k_l$  and  $n_l$  are the average of  $k$  and the number of  $\gamma$  rays in each part, respectively.

In the same manner as the case of the bremsstrahlung spectrum, the momentum of the target neutron was taken into account in the calculation. Assuming that each target neutron has the momentum distribution expected from the Hulthén wave function,<sup>10)</sup> the region of the neutron momentum between 0 MeV/c and 215 MeV/c was divided into 40 parts so that the number of the target neutron is equally distributed in each part.

(b) Five following quantities were chosen from random numbers.

- (1)  $\mathbf{P}$ : The initial momentum of the target neutron in the Lab. system.  $|\mathbf{P}|$  was determined by choosing one part from 40 parts described in (a). The angular distributions of  $\mathbf{P}$  were assumed to be isotropic.
- (2)  $\theta_{\pi}^{\text{CM}}$  and  $\varphi_{\pi}^{\text{CM}}$ : The production angle of the  $\pi^0$  meson in the center of mass system.  $\theta_{\pi}^{\text{CM}}$  was chosen from the region between  $\theta_{\pi\text{min}}^{\text{CM}} = \cos^{-1}(0.3)$  and  $\theta_{\pi\text{max}} = \cos^{-1}(-0.2)$ , because the reaction with  $\theta_{\pi}^{\text{CM}} < \theta_{\pi\text{min}}^{\text{CM}}$  or  $\theta_{\pi}^{\text{CM}} > \theta_{\pi\text{max}}^{\text{CM}}$  could not be detected kinematically.  $\varphi_{\pi}^{\text{CM}}$  was chosen in the region between  $0^\circ$  and  $360^\circ$ .

(c) The following quantities in the Lab. system were calculated for each  $k_l$  from the quantities determined in (b).

- (1)  $\mathbf{q}$ : The momentum of the produced  $\pi^0$  meson.
- (2)  $\mathbf{P}_n$ : The momentum of the recoil neutron.
- (3)  $k'$ : The energy of the incident of  $\gamma$  ray in the system in which the target neutron is at rest (corresponding to the energy of the  $\gamma$  ray in the Lab. system for the reaction  $\gamma + n \rightarrow \pi^0 + n$  when the neutron is free).

(d) Each calculated event was examined whether it could be detected by our experimental arrangement or not. For the event in which the recoil neutron could be detected, the detecting efficiency of the  $\pi^0$  mesons was calculated geometrically from  $\mathbf{q}$  and the arrangement of the  $\pi^0$  counter.

The processes from (b) to (d) were performed 7,000 times for each  $k_l$ . Then  $R$  is given by

$$R = 2\pi(\cos \theta_{\pi\text{min}}^{\text{CM}} - \cos \theta_{\pi\text{max}}^{\text{CM}})n_l \frac{\sum_{l=1}^{40} m_l}{M}, \quad (3.6)$$

where  $M$  is the number of times of the processes for  $k_l$  ( $M=7,000$ ) and  $m_l$  is the number of the detected events for  $k_l$ . Since the neutron counter was arranged at  $\theta_n = 34.8^\circ, 38.0^\circ, 41.2^\circ$  and  $47.6^\circ$ , the calculations were performed for each arrangement.

The reaction  $\gamma + d \rightarrow \pi^+ + n + (n)$  was measured to examine the validity of the present treatment for the internal motion of the target neutron in the deuteron. The experimental arrangement was the same as the calibration run of the neutron counter, except for the use of the liquid deuterium target. The  $\pi^+$  mesons with the momentum between 516.0 MeV/c and 552.0 MeV/c at  $\theta_{\pi} = 60^\circ$  were detected with the magnet system. The neutrons were detected in coincidence with the  $\pi^+$  mesons. The neutron counter was set at  $\theta_n = 37.7^\circ, 42.1^\circ, 45.0^\circ, 48.5^\circ$  and  $55.0^\circ$ , respectively. The setting angle of  $42.1^\circ$  corresponds to  $\theta_{\pi}^{\text{CM}} = 88^\circ$  of the reaction  $\gamma + p \rightarrow \pi^+ + n$  at  $k = 750$  MeV. As is shown in Fig. 8, the yields indicate that the angular spread of the recoil neutron from the deuteron target is wider than that expected from the proton target.

$R$  for the reaction  $\gamma+d \rightarrow \pi^+ + n + (n)$  can be calculated by the same procedure as  $R$  for the reaction  $\gamma+d \rightarrow \pi^0 + n + (p)$  by using  $\eta_{\pi^+}(\mathbf{q})$  in the place of  $\eta_{\pi^0}(\mathbf{q})$ .  $\eta_{\pi^+}(\mathbf{q})$  is the probability that the  $\pi^+$  mesons is detected. In order to obtain  $R$ 's for five arrangements, the processes of 1,040,000 times were performed for each arrangements.

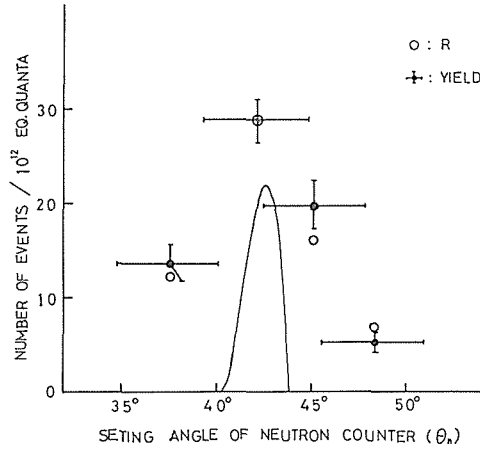


Fig. 8. Number of events of the reaction  $\gamma+d \rightarrow \pi^+ + n + (n)$ . The statistical error and the angular spread of the neutron are shown with bars. The solid curve shows the expected angular spread of the neutron in the case of the "at rest" target ( $\gamma+p \rightarrow \pi^+ + n$ ).  $R$ 's are normalized to the number of events at 42.1°.

Fig. 8 shows the yields and the calculated  $R$ 's for five arrangements.  $R$ 's are normalized to the number of events at 42.1°. The yields are in good agreement with  $R$ 's. The differential cross section at  $\theta_n=42.1^\circ$  was determined to be  $7.7 \mu\text{b/str}$  as the normalization factor. This value is in good agreement with M. Beneventano's data<sup>11)</sup> for the reaction  $\gamma+p \rightarrow \pi^+ + n$  within the experimental error. The procedure of the derivation of the cross section is proved to be adequate for the reaction

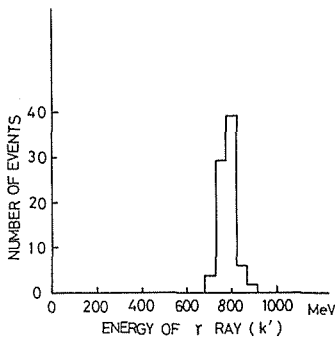


Fig. 9. The calculated energy spread of the  $\gamma$  rays for the reaction  $\gamma+d \rightarrow \pi^+ + n + (n)$  when the neutron counter was set at 42.1°. The scale of the abscissa corresponds to the energy of the incident  $\gamma$  ray in the Lab. system in which the target nucleon is at rest.

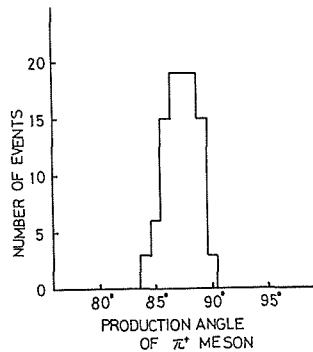


Fig. 10. The calculated angular spread for the reaction  $\gamma+d \rightarrow \pi^+ + n + (n)$  in the center of mass system when the neutron counter was set at 42.1°.

$\gamma + d \rightarrow \pi^+ + n + (n)$ . The calculated energy spread of the  $\gamma$  rays and angular spread of the  $\pi^+$  mesons for the arrangement of  $42.1^\circ$  are shown in Fig. 9 and Fig. 10, respectively.

b. Correction

1. Impulse approximation and multiple scattering

Assuming the impulse approximation and the closure approximation, Chew and Lewis<sup>12)</sup> gave the cross section of the  $\pi^0$  photoproduction from deuterons for nuclear recoil momentum  $Q$  as follows:

$$\frac{d\sigma}{dQ^2} \approx \frac{1}{2\pi} \left\{ \langle |\mathbf{K}_n|^2 \rangle_{AV} + \langle |\mathbf{K}_p|^2 \rangle_{AV} + \langle |L_n|^2 \rangle_{AV} + \langle |L_p|^2 \rangle_{AV} \right. \\ \left. + 2F(Q)Re \left[ \frac{1}{3} \langle |\mathbf{K}_n^* \cdot \mathbf{K}_p| \rangle_{AV} + \langle |L_n^* \cdot L_p| \rangle_{AV} \right] \frac{k - Q^2/2M}{2\nu_0} \right\},$$

where

$$F(Q) = \int \exp(i\mathbf{Q} \cdot \boldsymbol{\rho}) u_i^2(\boldsymbol{\rho}) d\rho \\ \boldsymbol{\rho} = \mathbf{r}_1 - \mathbf{r}_2.$$

$\langle |\mathbf{K}_n| \rangle_{AV}$  and  $\langle |L_n| \rangle_{AV}$ ; the spin flip and non spin flip cross section for a free neutron, respectively.

$\langle |\mathbf{K}_p| \rangle_{AV}$  and  $\langle |L_p| \rangle_{AV}$ ; the spin flip and non spin flip cross sections for a free proton, respectively.

$k$ ; the energy of the incident  $\gamma$  rays in the Lab. system

$\mathbf{r}_j$ ; the coordinates of the neutron or proton in the deuteron.

$u_i(\boldsymbol{\rho})$ ; the deuteron wave function

It is seen that the cross section for a deuteron is the sum of the cross sections of the free proton and neutron and the interference term. In the present experiment,  $Q \approx 700$  MeV/c and  $F(Q) \sim 10^{-2}$  therefore the interference term seems to be neglected as a small term.

In order to test the validity of the impulse approximation, M. Davier et al<sup>13)</sup> and J. I. Friedman and H. W. Kendall<sup>13)</sup> compared the experimental results of the coherent  $\pi^0$  photoproduction from the deuteron with the results of the impulse approximation calculation by Hadjoannou.<sup>14)</sup> At the  $\gamma$  ray energy region around the  $d(1236)$  resonance, the measured cross sections are fairly smaller than the calculated values and in agreement with Chappellear's calculations<sup>15)</sup> in which the rescattering corrections were taken into account. At around the  $\gamma$  ray energy of 500 MeV and  $Q \approx 500$  MeV/c, the experimental results agree with the impulse approximation calculation. The impulse approximation becomes more valid for the  $\pi^0$  photoproduction from the deuteron as the  $\gamma$  ray energy increases and as the transfer momentum increases. Therefore, the impulse approximation seems to be valid for our experiment ( $k=775$  MeV,  $Q=700$  MeV/c).

For the collision of high energy particles with the deuteron, the calculation on the effects due to the double scattering was performed by R. J. Glauber et al.<sup>16)</sup> The method is based on the presumption that the wavelength of the incident particle is much smaller than the ranges of the interaction with nucleons and that the interaction between the incident particle and the single nucleon is spin independent and spherically symmetric. They calculated the scattering cross section of the reaction  $\pi$ - $d$ ,  $K$ - $d$ ,  $p$ - $d$  and  $\bar{p}$ - $d$ , basing on the approximation that the scattering

nucleons are frozen in their instantaneous positions during the passage of the incident particle through the deuteron. The results give the good agreement with experimental results near the forward direction. However some disagreements are seen at large angles. A few authors attempted to extend the Glauber approach to larger angles. However, these calculations still seem to be unable to reproduce the experimental data. K. Schilling<sup>17)</sup> estimated the Glauber correction for the  $\pi^+$  photoproduction on the deuteron and obtained the value of about 6% for the small momentum transfer.

## 2. Multipion photoproduction

Although many measurements for the reaction  $\gamma + p \rightarrow \pi^- + \pi^+ + p$  have been performed, few measurements for other double pion photoproduction carried out. Our measurement arrangement could detect the double pion photoproduction in which one pion had the large momentum and the other had the small momentum. Since there is almost no experimental information on such a case, the correction for the double pion photoproduction was calculated with the assumption that there is no correlation in the final state. The correction was estimated to be less than 0.1%. Also the correction for the  $\eta$  photoproduction and the triple pion photoproduction are estimated to be negligibly small. Therefore, the correction for the multipion photoproductions was neglected.

### c. Experimental results

The data for the reaction  $\gamma + d \rightarrow \pi^0 + n + (p)$  at  $\theta_n = 41.2^\circ$  are shown in Fig. 11. The number of events for the reaction  $\gamma + d \rightarrow \pi^0 + n + (p)$  together with  $R$ 's calculated in the section § 3 a are shown in Fig. 12 and Table 3.  $R$ 's are normalized to the number of events at  $41.2^\circ$ . The number of events are in good agreement with  $R$ 's. Since  $\theta_{\pi}^{\text{CM}}$  and  $k$  for the experimental arrangement at  $38.0^\circ$  are nearly equal to those for  $41.2^\circ$  as is seen in Table 3, the weighted means of both data for  $38.0^\circ$  and  $41.2^\circ$  are listed in the last column of Table 3. The errors are summarized in Table 4. The measured cross section together with the calculated value by Yamaki's analysis are shown in Fig. 15. Fig. 13 and Fig. 14 show the calculated

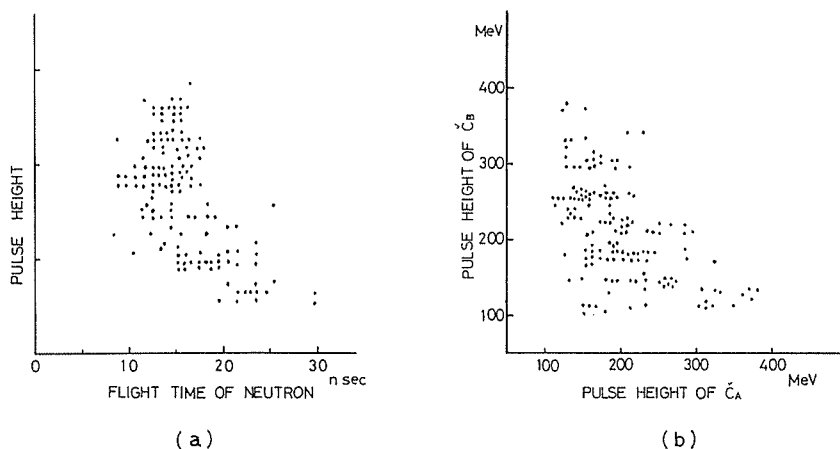


Fig. 11. Data for the reaction  $\gamma + d \rightarrow \pi^0 + n + (p)$  at  $\theta_n = 41.2^\circ$ . (a) shows two dimensional display of the flight time of the neutron and pulse height of the neutron counter. (b) shows two dimensional display of the pulse heights of the two Čerenkov counters. The energy scales correspond to the electron energy shown in Fig. 3.

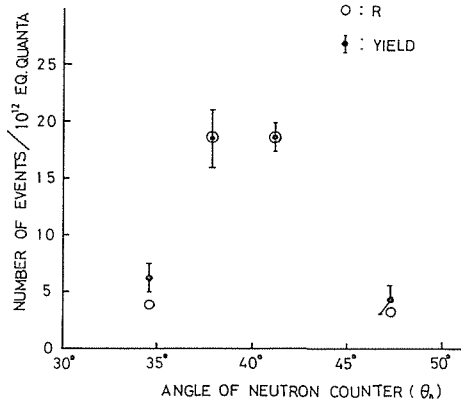


Fig. 12. Number of events of the reaction  $\gamma+d \rightarrow \pi^0+n+(p)$ . The error bars indicate the statistical error. The setting angle of  $41.2^\circ$  corresponds to  $\theta_{\pi}^{CM}=90^\circ$  for the reaction  $\gamma+p \rightarrow \pi^0+p$  at  $k=750$  MeV.  $R$ 's are normalized to the number of events at  $41.2^\circ$ .

Table 3. Cross sections for the reaction  $\gamma+n \rightarrow \pi^0+n$ .

Setting angle of neutron counter	34,8°	38,0°	41,2°	47,6°	38,0°+41,2°
number fo event par $10^{12}$ e.q.	6,52	18,4	18,7	4,8	18,6
$R$	$2,25 \times 10^{-3}$	$5,39 \times 10^{-3}$	$5,28 \times 10^{-3}$	$1,69 \times 10^3$	$5,31 \times 10^{-3}$
$\theta_{\pi}^{CM}$	$95,0^\circ \pm 2,0$	$91,0^\circ \pm 2,3^\circ$	$90,0^\circ \pm 2,2^\circ$	$86,0^\circ \pm 2,5^\circ$	$90,3^\circ \pm 2,6^\circ$
$k'$	$800 \pm 125$ MeV	$780 \pm 120$ MeV	$775 \pm 120$ MeV	$720 \pm 120$ MeV	$775 \pm 125$ MeV
$\frac{d\sigma}{d\Omega}$	$5,68 \mu\text{b/str}$	$6,69 \mu\text{b/str}$	$6,93 \mu\text{b/str}$	$5,51 \mu\text{b/str}$	$6,87 \pm 0,82 \mu\text{b/str}$

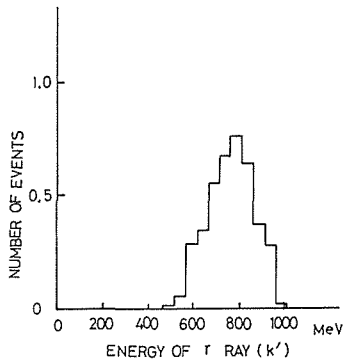


Fig. 13.

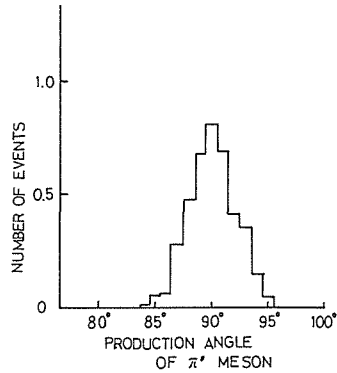


Fig. 14.

Fig. 13. The calculated energy spread of the  $\gamma$  rays for the reaction  $\gamma+d \rightarrow \pi^0+n+(p)$  when neutron counter and the  $\pi^0$  counter are set at  $\theta_n=41,2^\circ$  and  $\theta_\pi=62,6^\circ$ , respectively. The scale of the abscissa corresponds to the energy of the incident  $\gamma$  ray in the Lab. system in which the target nucleon is rest.

Fig. 14. The calculated angular spread of the reaction  $\gamma+d \rightarrow \pi^0+n+(p)$  in the center of mass system when the neutron counter and the  $\pi^0$  counter are set at  $\theta_n=41,2^\circ$  and  $\theta_\pi=62,6^\circ$ , respectively.

energy spread of the  $\gamma$  rays and the calculated angular spread of  $\pi^0$  mesons which could be detected with the experimental arrangement at  $41.2^\circ$ . The energy spread of the  $\gamma$  rays which are responsible for the reaction  $\gamma + n \rightarrow \pi^0 + n$  is about 250 MeV at FWHM. This spread is fairly larger than that for the reaction  $\gamma + d \rightarrow \pi^+ + n + (n)$ , because of the larger energy spread of the  $\pi^0$  counter than that of the analyzing magnet system for the  $\pi^+$  detection.

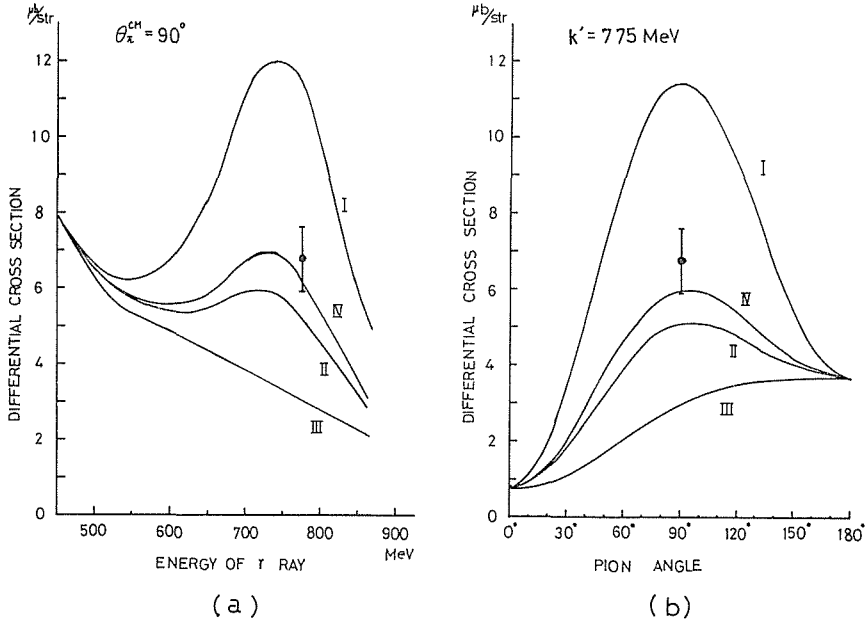


Fig. 15. Differential cross section of the reaction  $\gamma + n \rightarrow \pi^0 + n$ . The energy and angular spreads are shown in Fig. 13 and 14, respectively. The error is shown in Table IV.

The curves were calculated by Yamaki's analysis with the assumption that

Curve I:  $E_{2-S}/E_{2-V} = M_{2-S}/M_{2-V} = -1/3$ ,

Curve II:  $E_{2-S} = M_{2-S} = 0$  or  $E_{2-V} = M_{2-V} = 0$

Curve III:  $E_{2-S}/E_{2-V} = M_{2-S}/M_{2-V} = 1$

Curve IV:  $E_{2-S}/E_{2-V} = M_{2-S}/M_{2-V} = -1/11$ .

Table 4. Errors for the reaction  $\gamma + n \rightarrow \pi^0 + n$  at  $38.0^\circ$  and  $41.2^\circ$ .

statistical error	7.0 %
calculated solid angle	3.0 %
detecting efficiency of neutron counter	6.0 %
detecting efficiency of $\pi^0$ counter	3.0 %
maximum energy of $\gamma$ -rays	6.0 %
total error	12.0 %

The uncertainty of the quantameter is not included, since it has not been compared with others.

#### § 4. Discussion

In the energy region from 300 MeV to 850 MeV, T. Yamaki<sup>18)</sup> calculated phenomenologically the cross section and the polarization of the recoil nucleon

for the  $\pi^0$  photoproduction from the proton. He used the dispersion relation of Chew, Goldberger, Low and Nambu<sup>19)</sup> for the multipole amplitudes  $M_{1+}$ , and  $E_{0+}$  and the Breit-Wigner expressions for  $M_{1-}$ ,  $M_{2-}$  and  $E_{2-}$ .  $E_{1+}$  was neglected as the small term. The multipole amplitudes  $E_{2-}$  and  $M_{2-}$ , leading to the  $N(1518)$  resonance, are assumed as follows:

$$E_{2-} = iC_2 e f k q^2 \mu \frac{\eta_{13} e^{2i\delta_{13}} - 1}{q^5}, \quad (4.1)$$

$$M_{2-} = iC'_2 e f k^2 g^2 \frac{\eta_{13} e^{2i\delta_{13}} - 1}{q^5}, \quad (4.2)$$

with

$$\begin{aligned} C &= C_V \pm C_S & \left\{ \begin{array}{l} +: \text{ For } \gamma + p \rightarrow \pi^0 + p, \\ -: \text{ For } \gamma + n \rightarrow \pi^0 + n, \end{array} \right. \\ C' &= C'_V \pm C'_S \end{aligned}$$

where  $C_V$  (and  $C'_V$ ) and  $C_S$  (and  $C'_S$ ) are parameters corresponding to the isovector and isoscalar parts, respectively.  $C$  for the reaction  $\gamma + p \rightarrow \pi^0 + p$  is estimated to be  $-1.97$  by Yamaki. The definition of other notations is the same as the text.<sup>19)</sup> For the  $\pi N$  phase shifts three sets are used; a set derived by L. D. Roper<sup>20)</sup> and two sets by B. H. Bransden et al..<sup>21)</sup> The experimental data are in better agreement with the results obtained by using the set of Roper than the other sets. From the results of the analysis for the reaction  $\gamma + p \rightarrow \pi^0 + p$ , he concluded that the ratio  $M_{2-}/E_{2-}$  might be  $1/5 \sim 1/3$  and that five  $\pi N$  states,  $S_{11}$ ,  $S_{31}$ ,  $P_{11}$ ,  $P_{13}$  and  $D_{13}$ , were enough to account for the  $\pi^0$  photoproduction up to 850 MeV.

He calculated also the cross section for the coherent  $\pi^0$  photoproduction from the deuteron basing on the impulse approximation and assuming that

$$\text{Arg } M_{2-}^V - \text{Arg } M_{2-}^S = \text{Arg } E_{2-}^V - \text{Arg } E_{2-}^S = 0, \quad (4.3)$$

where the superscripts S and V indicate the isoscalar and isovector parts, respectively. It was concluded from the experimental results<sup>1)</sup> that the isotopic vector part was dominant in the  $D_{13}$  wave amplitude of the  $\pi^0$  photoproduction from free nucleons.

Yamaki also calculated the cross section for the reaction  $\gamma + n \rightarrow \pi^0 + n$ , using the Roper's  $\pi N$  phase shifts and  $M_{2-}/E_{2-} = 1/3$ . It is seen from Eqs. (1.2) and (1.4) that the cross section for the reaction  $\gamma + n \rightarrow \pi^0 + n$  can be calculated in the same way as for the reaction  $\gamma + p \rightarrow \pi^0 + p$  by changing the signs of the isoscalar parts of the multipole amplitudes. However, according to Yamaki's analysis, the isoscalar parts of  $M_{1+}$  and  $M_{1-}$  are neglected because of  $M^{S_{1+}}/M^{V_{1+}}$ ,  $M^{S_{1-}}/M^{V_{1-}} \sim 1/5$ .<sup>22)</sup> The calculation has been performed for various cases in which  $C_V + C_S = -1.97$ ,  $M_{2-}/E_{2-} = 1/3$  and  $C'_S/C'_V = C_S/C_V$ . In Fig. 15, the calculated results are shown together with the measured cross section. Four curves are calculated on the following assumption that

$$\text{Curve I: } E_{2-}^S/E_{2-}^V = M_{2-}^S/M_{2-}^V = -1/3 \quad (C_V = -1.97 \times 1.5, C_S = 1.97 \times 0.5)$$

$$\text{Curve II: } E_{2-}^S = M_{2-}^S = 0 \quad (C_V = -1.97, C_S = 0) \text{ or } E_{2-}^V = M_{2-}^V = 0 \\ (C_V = 0, C_S = -1.97)$$

$$\text{Curve III: } E_{2-}^S/E_{2-}^V = M_{2-}^S/M_{2-}^V = 1 \quad (C_V = C_S = -1.97 \times 0.5)$$

$$\text{Curve IV: } E_{2-}^S/E_{2-}^V = M_{2-}^S/M_{2-}^V = -1/11 \quad (C_V = -1.97 \times 1.1, C_S = 1.97 \times 0.1)$$

There is a little difference between the cross sections for  $E_{2-}^S = M_{2-}^S = 0$  and  $E_{2-}^V = M_{2-}^V = 0$ , due to the interference with other amplitudes. This difference is neglect-

ed in Curve II. In Curve III, the isoscalar part and isovector part of  $E_{2-}$  and  $M_{2-}$  are cancelled out. It is seen from Curve I and IV that a mixing of the isoscalar part with the opposite sign to the isovector part causes a rapid increase of the cross section for the reaction  $\gamma+n \rightarrow \pi^0+n$

It seems that the experimental result favors Curve II and IV rather than Curve I and III. This is consistent with the previous experimental result for the reaction  $\gamma+d \rightarrow \pi^0+d$  in which the isovector part was dominant. Therefore the experimental results support the dominant isovector part in the  $D_{13}$ -amplitude of the  $\pi$  photo-production from the nucleon around the  $N(1518)$  resonance.<sup>23)</sup>

#### ACKNOWLEDGEMENT

The author would like to express his sincere thanks to Professor S. Yasumi, Professor K. Miyake, Professor T. Nakamura and Professor S. Hatano for their continuous encouragement and stimulating discussion throughout this work. He wishes to thank Dr. R. Kikuchi, Mr. H. Okuno, Mr. Y. Hemmi and Mr. S. Kobayashi for their advice and collaboration in carrying out this experiment.

Thank are also due to the members of the synchrotron operation crew for their cooperative efforts.

#### REFERENCES

- 1) K. Miyake, K. Baba, S. Hatano, H. Itoh, M. Kihara, A. Masaike, T. Nakamura, M. Tamura, T. Yamaki, S. Yasumi and Y. Yoshimura: J. Phys. Soc. Japan **20** (1965) 1749.  
T. Nakamura, S. Hatano, Y. Hemmi, H. Itoh, M. Kihara, S. Kobayashi, K. Miyake, H. Okuno, T. Yamaki, S. Yasumi and Y. Yoshimura: J. Phys. Soc. Japan **24** (1968) 698.
- 2) K. M. Watson: Phys. Rev. **85** (1952) 852.
- 3) G. Cocconi and A. Silverman: Phys. Rev. **88** (1952) 1230.
- 4) C. R. Clinesmith, G. L. Hatch and A. V. Tollestrup: Proceedings of the International Symposium on Electron and Photon Interaction at High Energy at Hamburg Vol. II (1965) 245.
- 5) Y. Yoshimura, S. Hatano, Y. Hemmi, R. Kikuchi, S. Kobayashi, K. Miyake, T. Nakamura, H. Okuno and S. Yasumi: J. Phys. Soc. Japan **24** (1968) 1395.
- 6) Y. Hemmi, R. Kikuchi, S. Kobayashi, K. Miyake, T. Nakamura, H. Okuno, S. Yasumi and Y. Yoshimura: Nucl. Inst. and Meth. **59** (1967) 213.
- 7) The lead glass was manufactured by Ohara Optical Glass Co. Ltd., Kanagawa, Japan.
- 8) The scintillator was manufactured by Matsushita Electric Work, Ltd., Osaka, Japan.
- 9) D. G. Crabb, J. G. McEwen, E. G. Auld and A. Langsford: Nucl. Inst. and Meth. **48** (1967) 87.  
C. G. Wiegand, T. Elioff, W. B. Johnson, L. B. Auerbach, J. Lach and T. Ypsilantis: Rev. Sci. Instr. **33** (1962) 526.
- 10) D. H. White, R. M. Schectman and B. M. Chasan: Phys. Rev. **120** (1960) 614.  
E. Lohrman: DESY Report 67/40.
- 11) M. Beneventano, L. Paluzzi, F. Sebastiani, M. Severi and M. Grilli: to be published at Nuovo Cimento.
- 12) G. F. Chew and H. W. Lewis: Phys. Rev. **84** (1951) 779.
- 13) M. Davier, D. Benaksas, D. Drickey and P. Lehman: Phys. Rev. **137** (1964) B119.  
J. I. Friedman and H. W. Kendall: Phys. Rev. **129** (1963) 2803.
- 14) F. T. Hadjioannou: Phys. Rev. **125** (1962) 1414.
- 15) J. Chapplear: Phys. Rev. **99** (1955) 254.
- 16) R. J. Glauber: Phys. Rev. **100** (1955) 242.  
V. Franco and R. J. Glauber: Phys. Rev. **142** (1966) 1195,



- Phys. Rev. **156** (1968) 1685.
- 17) K. Schilling: DESY Report 68/35.
  - 18) T. Yamaki: Prog. Theor. Phys. **38** (1967) 153.
  - 19) G. F. Chew, M. L. Foldberger, F. E. Low and Y. Nambu: Phys. Rev. **106** (1957) 1345.
  - 20) L. D. Roper, R. M. Wright and B. T. Feld: Phys. Rev. **138** (1965) B190.
  - 21) B. H. Bransden, P. J. O'Donnell and R. G. Moorhouse: Phys. Rev. **139** (1965) B1566.
  - 22) A. Donnachie suggested that the strong enhancement of  $M_{1-}$  for the pion photoproduction from the neutron might appear from the constructive interference between the isoscalar part and the isovector part.
  - 23) A. Bietti suggested  $M_{2-}/E_{2-}=1/3$  and the dominance of the isovector amplitude in the transition between nucleon and the  $N(1518)$  resonance.